

# Improvement of Convergence in Moment-Method Solutions by the Use of Interpolants

MARK J. HAGMANN, STUDENT MEMBER, IEEE, OM P. GANDHI, SENIOR MEMBER, IEEE, AND CARL H. DURNEY, MEMBER, IEEE

**Abstract**—Two interpolants are described that may be used to correct the results of a moment-method solution using pulse functions as a basis and delta functions for testing. The interpolants allow for some of the variation of the fields within each cell and thereby increase accuracy and improve convergence. The interpolants are usable for a general scatterer and typically require about 1 percent of the cost of the initial numerical solution.

## I. INTRODUCTION

MOMENT-METHOD solutions for electromagnetic scattering with a general dielectric object often use pulse functions as a basis and delta functions for testing [1]–[5]. The object of this paper is to show that an interpolant may be used to allow for some of the variation of the fields within each cell and thereby increase accuracy and improve convergence. The computational expense of using the interpolant is typically about 1 percent of the cost of the initial numerical solution.

A numerical solution using a pulse function basis results in a single value representing  $\vec{E}$  within each cell. The delta functions used for testing enforce the integral equation at the center of each cell so that the calculated  $\vec{E}$  values are most representative of the cell centers. Experimental tests have shown that the error in  $\vec{E}$  calculated for the cell centers is relatively small even when adjacent cells have values which may differ by an order of magnitude [6]. Since the values of  $\vec{E}$  may be assigned to points in space, interpolation is possible.

The present study has been restricted to piece-wise interpolation in which the value of the corrected specific absorption rate (SAR) is calculated for one cell at a time. In this paper, two interpolants that have been developed by the authors are described. The triquadratic interpolant is usable when cell centroids are on a Cartesian product mesh. The NEWSUD interpolant is useful for problems in which the cubical cells may have different sizes and general locations.

Manuscript received September 20, 1977; revised January 12, 1978. This work was supported by the U.S. Army Medical Research and Development Command, Washington, DC, under Contract DAMD 17-74-C-4092.

The authors are with the Department of Electrical Engineering, Merrill Engineering Building, University of Utah, Salt Lake City, UT 84112.

## II. TEST OF A ONE-DIMENSIONAL INTERPOLANT

Moment-method solutions with any subsectional basis, such as pulse functions, require that the scatterer be approximated by a composite of cells [1]–[5]. Since analytical solutions for such composites are unknown in three-dimensional problems, a test of convergence has been made for a one-dimensional problem.

Consider the one-dimensional problem of a plane wave polarized in the  $x$  direction incident upon a dielectric slab which extends from  $z=0$  to  $z=a$ . The electric field is described by a scalar integral equation:

$$E_x(z) = E_x^i(z) - \frac{jk_0}{2} \int_0^a (\epsilon_r(z') - 1) E_x(z') e^{-jk_0 \rho} dz' \quad (1)$$

where  $z$  and  $z'$  are coordinates of the observation point and source point, respectively,  $\rho$  is the distance between the two points,  $E_x^i$  and  $E_x$  are the incident and total electric-field intensity, respectively, with  $e^{j\omega t}$  time dependence,  $\epsilon_r(z')$  is the complex permittivity at the source point relative to free space, and  $k_0 \equiv \omega \sqrt{\mu_0 \epsilon_0}$ .

The discrete analogue of (1) consists of the  $N$ -by- $N$  system of linear equations:

$$\sum_{n=1}^N A_{mn} E_{xn} = E_{xm}^i, \quad m=1, 2, \dots, N \quad (2)$$

where the dielectric is partitioned into  $N$  cells which are thin slabs, and  $n$  and  $m$  are indices for the cells.

The matrix elements are readily evaluated using (1) with the procedure in [2]:

$$A_{mn} = 1 + (\epsilon_{rn} - 1)(1 - e^{-jk_0 \Delta/2}) \quad (3)$$

$$A_{mn} = j(\epsilon_{rn} - 1) e^{-jk_0 \rho_{mn}} \sin\left(\frac{k_0 \Delta}{2}\right), \quad m \neq n \quad (4)$$

where  $\Delta$  is the thickness of each cell and  $\rho_{mn}$  is the distance between the centers of the  $m$ th and  $n$ th cells.

The analytical solution for a homogeneous dielectric slab is given by

$E_x(z)$

$$= \frac{E_x^i(0) [2\sqrt{\epsilon_r} \cos \sqrt{\epsilon_r} k_0(a-z) + 2j \sin \sqrt{\epsilon_r} k_0(a-z)]}{2\sqrt{\epsilon_r} \cos \sqrt{\epsilon_r} k_0 a + j(1+\epsilon_r) \sin \sqrt{\epsilon_r} k_0 a} \quad (5)$$

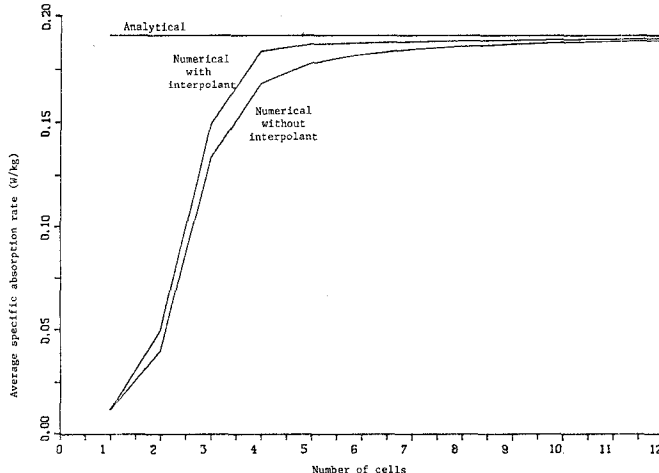


Fig. 1. Calculated average specific absorption rate for a 2-cm thick layer of muscle at 2450 MHz. Incident power density is 1 MW/cm<sup>2</sup>,  $\epsilon_r = 50$ ,  $\sigma = 2.2$  mho/m.

Fig. 1 gives the average SAR for a 2-cm thick layer of muscle at 2450 MHz for three different computational procedures. The analytical value was found by integration of  $1/2 \sigma \vec{E} \cdot \vec{E}^*$  using (5). Numerical solutions were obtained using (2)–(4). Numerical values without the interpolant were found by averaging  $1/2 \sigma \vec{E} \cdot \vec{E}^*$  for each cell. Numerical values were also obtained by using a piece-wise quadratic interpolant [7] to obtain an expression for  $\vec{E}$  within each cell and then integrating the expressions for a volume average of  $1/2 \sigma \vec{E} \cdot \vec{E}^*$ .

It is readily seen in Fig. 1 that the interpolant causes a significant improvement in convergence to the known analytical solution. We may relate the improvement in convergence to the well-known preference of Simpson's rule to the trapezoidal rule for numerical quadrature. Simpson's rule requires fitting a piecewise quadratic through the data points and generally gives a better approximation of the integrand function for greater accuracy than the trapezoidal rule.

### III. TRIQUADRATIC INTERPOLANT

We have developed a triquadratic interpolant which may be used when the cell centroids are on a Cartesian product mesh. As the name suggests, quadratic interpolation is used parallel to each of the three Cartesian axes.

A total of 27 cells is used in the stencil for each calculation. Fig. 2 shows the location of the 26 cells surrounding the cell in which the correction is made. The Cartesian product is shown for  $X = -1, 0, 1$ ,  $Y = -1, 0, 1$ ,  $Z = -1, 0, 1$ , but scaling is readily used to adjust to a specified cell size.

Quadratic interpolation may be used with univariate data for the function  $F(X)$  at the three points  $X = -1, 0, 1$  by the rule

$$F(X) = F(-1) \frac{X}{2} (X-1) + F(0)(1-X) \cdot (1+X) + F(1) \frac{X}{2} (X+1). \quad (6)$$

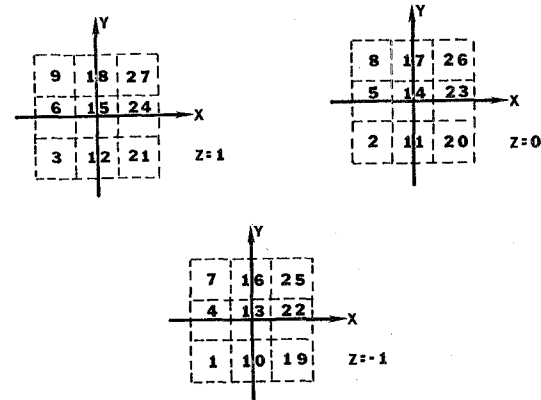


Fig. 2. Location of cells in stencil for the triquadratic interpolant.

Triquadratic interpolation may be performed on the stencil shown in Fig. 2 by using products formed from three univariate interpolants. For example, the contribution of the function value at  $X = -1, Y = -1, Z = 0$  (cell number 2) is

$$F(-1, -1, 0) \frac{X}{2} (X-1) \frac{Y}{2} (Y-1)(1-Z)(1+Z).$$

Triquadratic interpolation as described in the last paragraph is only usable for corrections in a cell surrounded by 26 other cells, as shown in Fig. 2. It is possible to use a single interpolation rule based on the full 27-cell stencil if  $\vec{E}$  values are estimated for unoccupied positions by means of a series of fill-in rules. We have used the following series of rules in which the  $\vec{E}$  values are filled in the order of increasing distance from the central cell by averaging  $\vec{E}$  values known in adjacent cells.

- 1) Fill in the six closest cells (numbers 5, 11, 13, 15, 17, 23). If any are unoccupied, use the value of  $\vec{E}$  in the central cell.
- 2) Fill in the twelve next closest cells (numbers 2, 4, 6, 8, 10, 12, 16, 18, 20, 22, 24, 26). If any are unoccupied, use one-half the sum of  $\vec{E}$  for the pair from the six closest cells of part 1 which share a face with the unoccupied cell.
- 3) Fill in the eight corner cells (numbers 1, 3, 7, 9, 19, 21, 25, 27). If any are unoccupied, use one third the sum of  $\vec{E}$  for the three cells sharing a face with the unoccupied cell.

Application of triquadratic interpolation to the general scatterer requires the following calculations be made for each cell. First, a sieve is used to find which of the 26 surrounding cells are occupied. Next, the fill-in rules are used as required to complete the stencil. Finally, the triquadratic interpolant is used to evaluate the integral of  $1/2 \sigma \vec{E} \cdot \vec{E}^*$  over the central cell. If the cells have different complex permittivities, both the fill-in and interpolation rules must be modified by suitably multiplying by the ratio of permittivities so that the interpolant has both  $\vec{D}$  normal and  $\vec{E}$  tangential to each boundary continuous. We have made such modifications and have used interpolation in solutions for inhomogeneous dielectric scatterers.

Since analytical solutions are not available for arrays of cubes, a standard for evaluating results obtained by

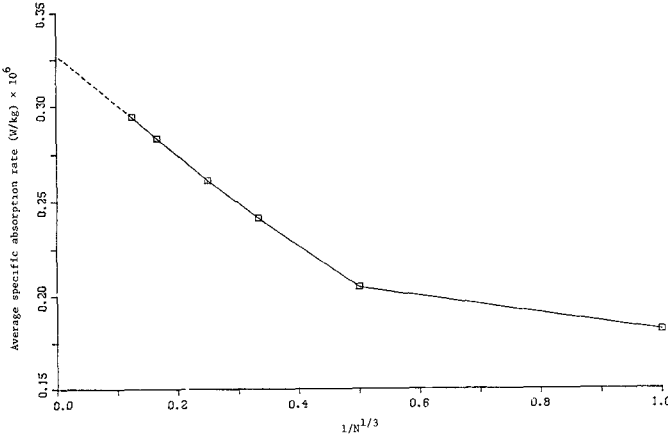


Fig. 3. Calculated average specific absorption rate for a 12-cm cube of muscle at 1 MHz without interpolation. Incident power density is 1 MW/cm<sup>2</sup>,  $\epsilon_r = 2000$ ,  $\sigma = 0.556$  mho/m.

TABLE I  
ERROR IN CALCULATED AVERAGE SPECIFIC ABSORPTION RATE  
FOR A 12-cm CUBE OF MUSCLE AT 1 MHz.  $\epsilon_r = 2000$ ,  $\sigma = 0.556$   
mho/m

Number of Cells	Error Without Interpolant	Error With Interpolant
1	-44.6%	-44.6%
8	-37.4%	-34.4%
27	-26.3%	-20.9%
64	-20.2%	-15.4%
216	-13.5%	-9.01%
512	-10.1%	-5.89%

numerical methods is not easily obtained, but one convergence test has been made for the triquadratic interpolant. Fig. 3 gives the average specific absorption rate calculated without interpolation for a 12-cm cube of muscle with plane wave at 1 MHz normally incident on one face. Linear convergence is demonstrated in the figure. Extrapolation using the values for 216 and 512 cells gives an SAR of  $0.3275 \times 10^{-6}$  W/kg for an incident power density of 1 MW/cm<sup>2</sup>. Table I gives the estimated errors in SAR without interpolation and with the triquadratic interpolant found by comparison with the extrapolated value of SAR. Results in Table I suggest that the triquadratic interpolant causes a significant improvement in convergence.

#### IV. NEWSUD INTERPOLANT

We have developed the NEWSUD interpolant which may be used when the cells have different sizes and/or arbitrary placement. The NEWSUD interpolant is more general than the triquadratic interpolant and does not require fill-in rules but is limited to linear rather than quadratic correction. The name NEWSUD is an acronym of the words "north," "east," "west," "south," "up," and

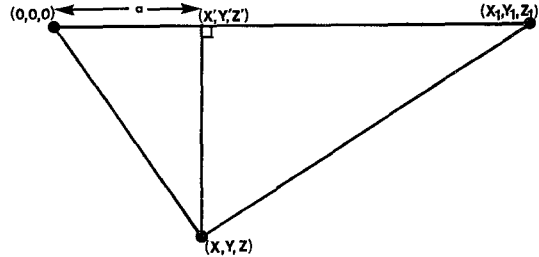


Fig. 4. Configuration for linear interpolation in the NEWSUD method.

"down" since the stencil contains only one cell near each of the six faces of a central cube for calculations within that cube.

When the NEWSUD interpolant is used for calculations within a cell, first, one imaginary plane is passed through each edge of the cube and the cell centroid. The planes divide the cube into six congruent pyramids as well as dividing the exterior into six corresponding solid angles. Next, each solid angle is searched to find a cell centroid as close as possible to the interpolated cube. Interpolation is performed separately in each of the six pyramids using only the centroids of the interpolated cube and corresponding external cell. If a solid angle does not contain an external cell centroid within a reasonable distance, say one side of the central cell or less, the uninterpolated value of  $\vec{E}$  is used within the corresponding pyramid.

The configuration for linear interpolation within a pyramid in the NEWSUD method is shown in Fig. 4. The point at which interpolation is desired  $(X, Y, Z)$ , the centroid of the external cell  $(X_1, Y_1, Z_1)$ , and the centroid of the interpolated cell which is used as the origin determine a plane which is used for the figure.

The equation of the plane perpendicular to the line connecting  $(X_1, Y_1, Z_1)$  to the origin and passing through the point  $(X, Y, Z)$  is

$$XX_1 + YY_1 + ZZ_1 = a\sqrt{X_1^2 + Y_1^2 + Z_1^2} \quad (7)$$

where  $a$  is the distance from the origin to the plane. The linear interpolation used in the NEWSUD method when an external cell is found corresponding to a pyramid of the interpolated cell is accomplished by the approximation of identifying  $\vec{E}(X, Y, Z)$  with  $\vec{E}(X', Y', Z')$  so that

$$\vec{E}(X, Y, Z) = \frac{a\vec{E}(X_1, Y_1, Z_1)}{\sqrt{X_1^2 + Y_1^2 + Z_1^2}} + \left[ 1 - \frac{a}{\sqrt{X_1^2 + Y_1^2 + Z_1^2}} \right] \vec{E}(0, 0, 0). \quad (8)$$

Linear interpolation defined by (7) and (8) is used to evaluate the integral of  $1/2 \sigma \vec{E} \cdot \vec{E}^*$  in a pyramid for which a corresponding external cell is found. If the cells have different complex permittivities, (8) must be modified by suitably multiplying by the ratio of permittivities

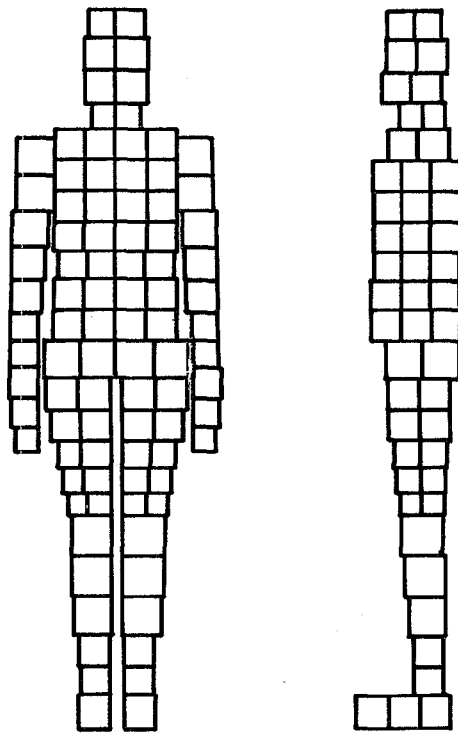


Fig. 5. An improved model of man for numerical calculations.

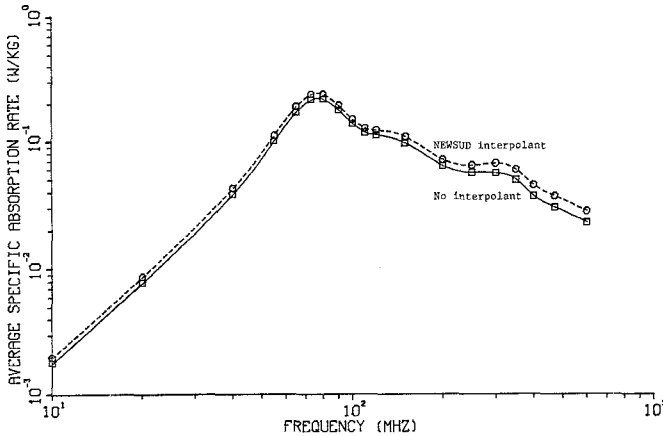


Fig. 6. Whole-body SAR for a homogeneous model of man.  $\vec{E} \parallel \hat{L}$ ,  $\vec{k}$  front-to-back, incident intensity = 1 MW/cm<sup>2</sup>.

so that both  $\vec{D}$  normal and  $\vec{E}$  tangential to a boundary are continuous.

Fig. 5 illustrates a model of man which has been used for numerical calculations [8]. Moment-method solutions have been made for the model using pulse functions as a basis and delta functions for testing. The NEWSUD interpolant has been used in calculations since the model has cells which are cubes of different sizes. Fig. 6 shows the frequency dependence of the average SAR calculated for the model of man with a vertically polarized plane wave having frontal incidence. Values found both with and without interpolation are given.

If the local  $\vec{E}$  values are exact samples and if there is appreciable variation between adjacent cells, then statistical procedures may be used to calculate confidence limits

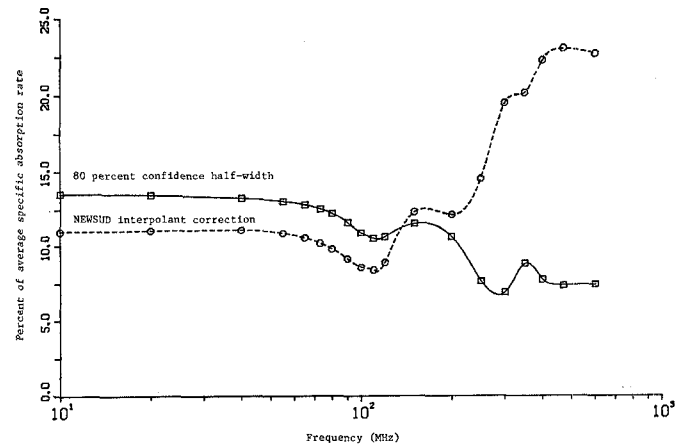


Fig. 7. Correction to whole-body SAR for homogeneous model of man.

for values of the average SAR found without aid of interpolants [9]. The 80-percent confidence half widths for average SAR values have been calculated and plotted in Fig. 7. The percent correction which the NEWSUD interpolant makes is also shown in Fig. 7.

The frequency-dependent variation of the true  $\vec{E}$  must cause increasing error in calculations of local  $\vec{E}$  at frequencies greater than 200 MHz for the cell sizes used with the model of man [10]. The 80-percent confidence half widths shown in Fig. 7 are not valid at frequencies above 200 MHz since their calculation requires the assumption that the local  $\vec{E}$  values are exact samples. Fig. 7 shows that the NEWSUD interpolant makes relatively little correction to the SAR at low frequencies where relatively little error is expected, but the correction increases sharply at frequencies for which the error is expected to increase.

## V. CONCLUSIONS

The interpolative correction to calculated values of the average SAR has been tested in a one-dimensional problem in which the analytical solution is available for comparison with numerical solutions. A test was also made in a three-dimensional problem in which the true solution was estimated by extrapolation. In both tests the interpolant makes small corrections when few cells are used since sampling is insufficient to allow proper estimation of the variation of the fields. The fractional correction is also observed to decrease as many cells are used since the interpolated and uninterpolated solutions must converge to the same answer. In both tests the interpolant was found to provide a significant reduction in error for a negligible increase in computational expense.

It is hoped that the two interpolants presented in this paper are only the first steps in the development of a procedure which will find general usage as a follow-up to moment-method solutions. Use of the interpolant for calculation of the external scattered fields and development of a general interpolant consistent with the wave equation appear to be the next necessary steps.

## REFERENCES

- [1] J. H. Richmond, "Scattering by a dielectric cylinder of arbitrary cross section shape," *IEEE Trans. Antennas Propagat.*, vol. AP-13, pp. 334-341, May 1965.
- [2] —, "TE-wave scattering by a dielectric cylinder of arbitrary cross-section shape," *IEEE Trans. Antennas Propagat.*, vol. AP-14, pp. 460-464, July 1966.
- [3] G. W. Hohmann, "Three-dimensional induced polarization and electromagnetic modeling," *Geophysics*, vol. 40, pp. 309-324, Apr. 1975.
- [4] D. E. Livesay and K. M. Chen, "Electromagnetic fields induced inside arbitrarily shaped biological bodies," *IEEE Trans. Microwave Theory Tech.*, vol. MTT-22, pp. 1273-1280, Dec. 1974.
- [5] R. F. Harrington, *Field Computation by Moment Methods*. New York: Macmillan, 1968.
- [6] B. S. Guru and K. M. Chen, "Experimental and theoretical studies on electromagnetic fields induced inside finite biological bodies," *IEEE Trans. Microwave Theory Tech.*, vol. MTT-24, pp. 433-440, July 1976.
- [7] P. J. Davis, *Interpolation and Approximation*. New York: Dover, 1975.
- [8] M. J. Hagmann, O. P. Gandhi, and C. H. Durney, "Numerical calculation of electromagnetic energy deposition for a realistic model of man," presented at the 1977 USNC/URSI Meeting, Airlie, VA.
- [9] W. Mendenhall and R. L. Schaeffer, *Mathematical Statistics with Applications*, North Scituate, MA Duxbury, 1973.
- [10] M. J. Hagmann, O. P. Gandhi, and C. H. Durney, "Upper bound on cell size for moment-method solutions," *IEEE Trans. Microwave Theory Tech.*, vol. MTT-25, pp. 831-832, Oct. 1977.

# Aperture Excitation of a Wire in a Rectangular Cavity

DAVID B. SEIDEL, MEMBER, IEEE

**Abstract**—The problem of determining the currents excited on a wire enclosed within a rectangular cavity is considered. The wire and cavity interior are excited by electromagnetic sources exterior to the cavity which couple to the cavity interior through a small aperture in the cavity wall. It is assumed that the wire is thin, straight, and oriented perpendicular to one of the cavity walls. An integral equation is formulated for the problem in the frequency domain using equivalent dipole moments to approximate the effects of the aperture. This integral equation is then solved numerically by the method of moments. The dyadic Green's functions for this problem are difficult to compute numerically; consequently, extensive numerical analysis is necessary to render the solution tractable. Sample numerical results are presented for representative configurations of cavity, wire, and aperture.

## I. INTRODUCTION

**A**N INVESTIGATION has been undertaken of the problem of a wire inside a cavity which is excited by an external source. The effects of this external source are coupled to the cavity interior and wire through an aperture in the cavity wall. The currents excited upon the wire and the fields within the cavity are to be determined. This boundary-value problem is an idealization of a wire in some metal enclosure. As examples, the wire may be inside the shielding or housing of an electronic or

mechanical unit, or it might simply pass from one metal partition to another through a region which is essentially empty.

Previously, the shielding effects of infinite cylindrical structures have been treated often, i.e., [1], [2]. Recently, the problems of penetration through an aperture into a spherical cavity [3] and into a cylindrical cavity [4] also have been considered. However, the author is not aware of any previous work which treats the subsequent interaction with scatterers (such as wires) within a cavity.

## II. FORMULATION OF PROBLEM

For purposes of this problem, consider a perfectly conducting rectangular cavity as shown in Fig. 1. One corner of this cavity is located at the origin of a Cartesian coordinate system. The dimensions of the cavity are denoted by  $a$ ,  $b$ , and  $c$ , in the  $x$ ,  $y$ , and  $z$  directions, respectively. Within this cavity, there is a perfectly conducting, round, thin wire of radius  $r$  ( $r \ll \lambda$ ) which is assumed to be parallel to the  $z$  axis. The ends may or may not be attached to either or both walls of the cavity.

One of the walls of the cavity is perforated by a small aperture whose center is located at  $\bar{r}_a = (x_a, y_a, z_a)$ . The exterior region to which the aperture couples the cavity interior may be of two different types. The cavity may be located behind an infinite, perfectly conducting, planar screen such that the cavity wall containing the aperture is a portion of the infinite screen. Alternatively, the cavity

Manuscript received October 21, 1977; revised March 1, 1978. This work was supported by the Air Force Office of Scientific Research Air Force Systems Command, USAF, under Grant AFOSR 76-3009.

The author was with the University of Arizona, Tucson, AZ. He is now with the Cooperative Institute for Research in Environmental Sciences, University of Colorado/NOAA, Boulder, CO 80309.